Cellular Physiology and Biochemistry

Cell Physiol Biochem 2020;54:211-229
DOI: 10.33594/000000215
Published online: 27 February 2020
Accepted: 10 February 2020

Original Paper

ATP Synthase Subunit *a* Supports Permeability Transition in Yeast Lacking Dimerization Subunits and Modulates yPTP Conductance

Katarzyna Niedzwiecka Emilia Baranowska Chiranjit Panja Roza Kucharczyk

Institute of Biochemistry and Biophysics, Polish Academy of Sciences, Warsaw, Poland

Key Words
Mitochondria • Permeability transition pore • ATP synthase • *ATP6* • Subunit *a* • *S. cerevisiae*

Abstract
Background/Aims: Mitochondrial ATP synthase, in addition to being involved in ATP synthesis, is involved in permeability transition pore (PTP) formation, which precedes apoptosis in mammalian cells and programmed cell death in yeast. Mutations in genes encoding ATP synthase subunits cause neuromuscular disorders and have been identified in cancer samples. PTP is also involved in pathology. We previously found that in *Saccharomyces cerevisiae,* two mutations in ATP synthase subunit *a* (*atp6-P163S* and *atp6-K90E*, equivalent to those detected in prostate and thyroid cancer samples, respectively) in the *OM45-GFP* background affected ROS and calcium homeostasis and delayed yeast PTP (yPTP) induction upon calcium treatment by modulating the dynamics of ATP synthase dimer/oligomer formation. The Om45 protein is a component of the porin complex, which is equivalent to mammalian VDAC. We aimed to investigate yPTP function in *atp6-P163S* and *atp6-K90E* mutants lacking the *e* and *g* dimerization subunits of ATP synthase. ***Methods:*** Triple mutants with the *atp6-P163S* or *atp6-K90E* mutation, the *OM45-GFP* gene and deletion of the *TIM11* gene encoding subunit *e* were constructed by crossing and tetrad dissection. In spores capable of growing, the original *atp6* mutations reverted to wild type, and two compensatory mutations, namely, *atp6-C33S-T215C,* were selected. The effects of these mutations on cellular physiology, mitochondrial morphology, bioenergetics and permeability transition (PT) were analyzed by fluorescence and electron microscopy, mitochondrial respiration, ATP synthase activity, calcium retention capacity and swelling assays. ***Results:*** The *atp6-C33S-T215C* mutations in the *OM45-GFP* background led to delayed growth at elevated temperature on both fermentative and respiratory media and increased sensitivity to high calcium ions concentration or hydrogen peroxide in the medium. The ATP synthase activity was reduced by approximately 50% and mitochondrial network was hyperfused in these cells grown at elevated temperature. The *atp6-C33S-T215C* stabilized ATP synthase dimers and restored the yPTP properties in *Tim11Δ*

Roza Kucharczyk
Institute of Biochemistry and Biophysics
Polish Academy of Sciences, Warsaw (Poland)
Tel. 48 22 5921221, Fax 48 22 6584636, E-Mail roza@ibb.waw.pl

cells. In *OM45-GFP* cells, in which Tim11 is present, these mutations increased the fraction of swollen mitochondria by up to 85% vs 60% in the wild type, although the time required for calcium release doubled. ***Conclusion:*** ATP synthase subunit *e* is essential in the *S. cerevisiae atp6-P163S* and *atp6-K90E* mutants. In addition to subunits *e* and *g*, subunit *a* is critical for yPTP induction and conduction. The increased yPTP conduction decrease the *S. cerevisiae* cell fitness.

Introduction

Mitochondrial ATP synthase, an enzyme that provides cellular energy in the form of ATP, is composed of 17 subunits [1]. The intersubunit interactions are critical for the catalytic activity of the enzyme. These subunits form two main enzyme domains: the hydrophobic F_0 domain that embeds the enzyme in the inner mitochondrial membrane (IMM) and the catalytic F_1 domain that is exposed in the matrix [2]. ATP synthase uses a proton gradient established by the respiratory chain across the IMM. The higher concentration of protons in the intermembrane space (IMS) than in the matrix enables ATP synthase to produce ATP from ADP and inorganic phosphate [3]. Protons pass through the channel in the F_0 domain formed between the *c*-ring (consisting of ten *c* subunits in *Saccharomyces cerevisiae*) and the hydrophilic amino acids of subunit *a* (which is tightly attached to the *c*-ring), driving the rotation of the ring. The proton enters from the IMS into the entry half-channel. It binds to an acidic residue (*c*E58 in *S. cerevisiae*) in the second helix of subunit *c* and, after an almost complete rotation of the ring, is liberated to the exit half-channel on the matrix side [4, 5]. The *c*-ring is tightly bound to the central stalk subunits *γ, δ,* and *ε*, of which subunit *γ* protrudes into the F_1 catalytic domain (composed of a hexamer of *α* and *β* subunits). Subunit *γ* rotates with the ring and induces cyclic conformational changes in F_1 [6, 7]. Consequently, ADP and Pi are sequentially converted to ATP at the catalytic sites of *β* subunits, according to the binding change mechanism. In addition to subunits *a* and *c*, the F_0 domain consists of hydrophobic subunits *8*, *i/j*, and *f* and the membrane part of subunit *b*. The hydrophilic part of *b* protrudes into the matrix, interacts with the *d*, *h*, and *OSCP* (oligomycin sensitivity-conferring protein) subunits and forms the external stalk that connects F_0 with F_1. Three additional subunits, namely, *e*, *g*, and *k*, stabilize the ATP synthase dimers [8] that self-assemble in longer ribbons that are important for cristae formation [9, 10].

In addition to its main function in ATP production, IMM curvature and the formation of the mitochondrial network [11], ATP synthase has been proposed to be directly involved in the permeability transition (PT) [12-14]. PT is a Ca^{2+}-dependent increase in IMM permeability to solutes and proteins with an exclusion limit of approximately 1500 Da due to the formation of the unselective high-conductance permeability transition pore (PTP), also called the mitochondrial megachannel (MMC) [15]. The PTP can open for a short duration and assume a low conductance, probably contributing to Ca^{2+} homeostasis and ROS signaling [16, 17], or can open for a long period with a high conductance, contributing to cell death [15]. A molecular explanation for this complex behavior of PTP, both in regulation and channel composition, has not been provided. Understanding PTP function and regulation is a major goal for scientists performing basic research and for clinicians because its dysregulation is implicated in pathological conditions such as neurodegeneration, cancer, cardiac hypertrophy and ischemia [18, 19]. The molecular composition of the channel remains a subject of debate [20, 21]. ATP synthase dimers or tetramers (but not monomers) eluted from native gels and reconstituted into liposomes form channels characterized by different conductances depending on the model organism [14, 22-24]. Similar experiments performed on the purified enzyme embedded in vesicles showed high-conductance channel activity for the tetramers, the dimers and the monomers [25, 26]. It was also proposed that PTP opening requires the dissociation of ATP synthase dimers [27]. Well characterized modulators of the PTP have been identified to bind to and act on subunits of ATP synthase, further corroborating its role as the molecular identity of the PTP. The divalent Mg^{2+}, Mn^{2+},

Sr^{2+} or Ba^{2+} cations have inhibitory effects on the PTP because they compete with Ca^{2+} to bind the catalytic site in the *β* subunit [28]. The specific PTP inducer Bz423 and the PTP regulator protein CyPD bind to *OSCP,* and at the same time, the inhibitory effect of matrix H^+ at a pH of 6.5 is achieved through the protonation of the unique histidine in the OSCP subunit [14, 29, 30]. Importantly, it was recently shown that deletion of the *c* subunit prevents the assembly of a functional ATP synthase [20]. This leads to loss of the PTP in mammalian cells, providing a strong argument in favor of PTP formation by ATP synthase or its specific subunits [27, 31].

Experiments in *S. cerevisiae* have also provided data supporting the role of ATP synthase in the formation of the yeast PTP (yPTP, also called the yeast mitochondrial unspecific channel, YMUC). Importantly, the features of the yPTP are similar to those of the mammalian PTP, i.e., regulation by calcium, ROS, and matrix cyclophilin D and involvement in cell death [22, 32, 33]. A unique feature of yeast ATP synthase is the presence of a cysteine at position 23 of the *a* subunit (Fig. 1). The disulfide bond formed between the cysteine residues of two neighboring *a* subunits stabilizes the ATP synthase dimer even in the absence of subunits *e, g* and *k*, as shown by BN-PAGE analysis of ATP synthase complexes isolated from mitochondria incubated with Cu^{2+} [34, 35]. The mitochondria of *S. cerevisiae* cells lacking subunits *e* and *g* are desensitized to calcium but are able to form a long-lasting channel with 10 times lower conductance than that of the wild-type channel. This permits calcium release but not swelling, which requires the high-conductance channel to be formed [22, 32, 35]. The first transmembrane domain of subunit *b* also plays a role in the stabilization of the open state of the yPTP [35].

We have previously shown that mutations in the mitochondrial *ATP6* gene of *S. cerevisiae*, namely, *atp6-P163S* and *atp6-K90E*, leading to the substitution of proline 153 for serine or lysine 80 for glutamic acid in subunit *a*, respectively (positions in mature subunit *a* after the removal of the first ten amino acids in the presequence by the protease Atp23 [36]), desensitized the yPTP to calcium in mitochondria bearing the Om45 protein fused to GFP. Importantly, these two *atp6* mutations were identified in prostate and thyroid cancer samples and may contribute to cell immortalization by facilitating escape from apoptosis [37]. The Om45 protein forms a complex with porin and interacts physically with the components of the IMM: transporters, adenine nucleotides carrier, respiratory chain complexes III and IV and ATP synthase [38]. It was proposed that this protein coordinates transport across mitochondrial membranes. In this study, we asked whether the *atp6-P163S* or *atp6-K90E* mutations influence the induction of the yPTP in mitochondria defective in ATP synthase dimerization, i.e., lacking subunits *e* and *g*. Surprisingly, we found that subunit *e* is essential

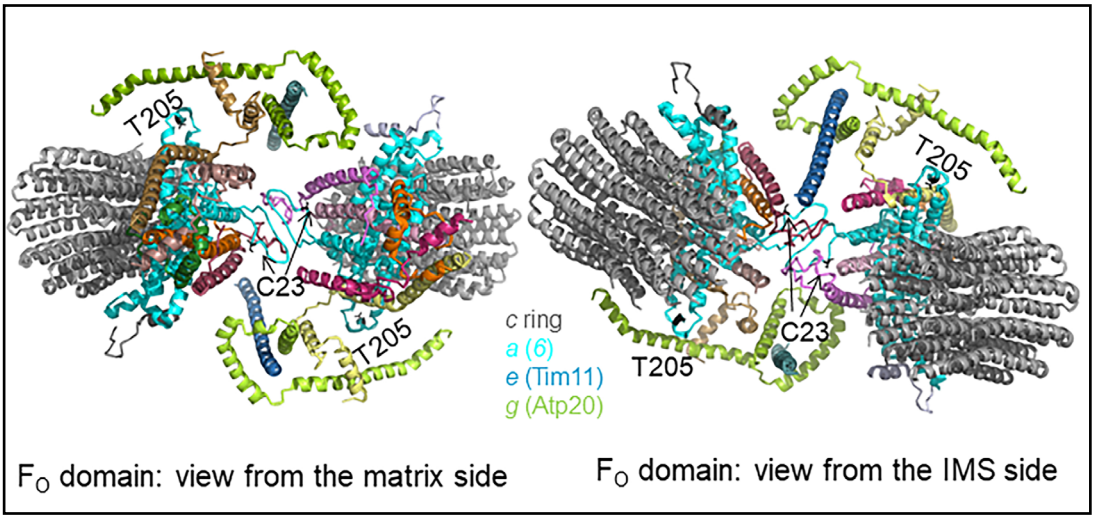

Fig. 1. Location of C23 and T205 residues in subunit *a* within the dimeric F_0 complex of S. cerevisiae. The Fig. was generated using the PDB 6B2Z structure obtained by H. Guo, S. Bueler and J. Rubinstein [1]. Both residues are located in the loops between α-helices and are represented as sticks.

in the *atp6-P163S* and *atp6-K90E* mutants. We show that subunit *a* of ATP synthase plays a role in yPTP induction and conduction and provide the first *in vivo* evidence that yPTP function is important for the fitness of *S. cerevisiae* cells.

Materials and Methods

Yeast strains

The *S. cerevisiae* strains used in this study were all isogenic derivatives of MR6 and are listed in Table 1. ρ+ indicates the complete wild-type mitochondrial genome (mtDNA; when followed by a mutation, it indicates the complete mtDNA with a single introduced mutation), and ρ^0 indicates the strain lacking mitochondrial DNA. The RKY62*α* and RKY61*α* strains were obtained by changing the mating type using a plasmid encoding the HO endonuclease [39]. The KNY58 strain was constructed by integrating the *tim11Δ::HphNTI* cassette into the *TIM11* locus of the MR6 strain. The cassette was amplified using the pMW77/11 plasmid as a template [40] with the following primers: 5′CACAGAAATTTTAGATAAAAGGAAGTATTATATCGGAACATAACGTATATAGGAA CTAGCGAGTGAGTTAAAGGATGGGTAAAAAGCCTGAACTCACCG3′ and 5′ATCCATCATAACTTCGTCATTCAGTG CGAGCTAATGTGCATTTTTAGTATCCTATTTATGTTGAAGCTTCTATTTTATTCCTTTGCCCTCGGACGAGTGC3′. The KNY67 strain was obtained by fusing *GFP* to the *3′* end of *OM45* in its genomic locus in the KNY58 strain, according to [41]. Thus, all strains expressed Om45-GFP under the control of the *OM45* gene promoter. The KNY58, KNY67 and MR6-OM45GFP strains were depleted of mtDNA by culturing them in liquid YPGalA medium at 37 °C and selecting respiration-deficient clones, yielding KNY59, KNY67-1 and KNY40, respectively. The absence of mtDNA in these clones was confirmed by crossing with the RKY25 *MATα* (a [ρ^+] strain bearing a point mutation in the *ATP6* gene that confers respiratory deficiency [42]). The diploid strains KNY68 and KNY70 were obtained by mating RKY61α with KNY59 and KNY67-1, respectively. The diploid strains KNY68 and KNY71 were obtained by mating RKY62α with KNY59 and KNY67-1, respectively. The KNY76-1 strain was obtained by sporulation and tetrad dissection of KNY68. The KNY88 diploid strain was obtained by mating KNY76-1 with KNY40. The KNY89-1 and KNY91-1 strains were obtained by sporulation of the KNY88 strain and subsequent tetrad dissection. The KNY103-1 strain was obtained by fusing G*FP* to the *OM45* gene in the KNY76-1 strain [41]. The absence of the Tim11 protein and the presence of the GFP tag at the C-terminus of the Om45 protein were confirmed by Western blot analysis using an anti-Tim11 antibody and GFP fluorescence, respectively. The sequence of the *ATP6* gene was verified by sequencing in all haploid strains with oAtp6-1 5′TAATATACGGGGGTGGGTCCCTCAC3′ and oATP6-10 5′GGGCCGAACTCCGAAGGAGTAAG3′, which were also used for *ATP6* gene amplification.

Growth conditions

Strains were grown in rich YPGA medium (1% Bacto yeast extract, 1% Bacto peptone, 2% glucose, 40 mg/l adenine) at 28 or 36 °C with shaking at 200 rpm. For mitochondrial isolation, strains were grown in rich YPGalA medium (1% Bacto yeast extract, 1% Bacto peptone, 2% galactose, 40 mg/l adenine) to an OD_{600} of 4. Respiratory YPGlyA medium contained 1% Bacto yeast extract, 1% Bacto peptone, 2% glycerol, and 40 mg/l adenine (Difco, Becton Dickinson). W0 complete minimal medium contained 6.7% yeast nitrogen base w/o amino acids and 2% galactose, supplemented with appropriate drop-out amino acid stock (Sunrise) for plasmid selection. The liquid media were solidified by addition of 2% Bacto agar (Difco, Becton Dickinson). An OD_{600} of 1 corresponds to 1.2 x 10^7 cells/ml for the MR6 strain. Geneticin or hygromycin were added to YPGA at a concentration of 200 μg/ml or 300 μg/ml, respectively.

Measurement of oxygen consumption and ATP synthase activity

Mitochondria were isolated from cells grown in YPGalA medium at 28 °C according to the protocol described in reference [43]. Oxygen consumption rates were measured using a Clarke electrode in respiration buffer (0.65 M mannitol, 0.36 mM EGTA, 5 mM Tris-phosphate, 10 mM Tris-maleate pH=6.8) after consecutively adding 75 μg of mitochondrial proteins, 4 mM NADH (state 4 respiration), 150 μM ADP (state 3) or 4 μM carbonyl cyanide m-chlorophenylhydrazone (CCCP) (uncoupled respiration), as previously described [44]. The rates of ATP synthesis were determined under the same experimental conditions with 750 μM ADP; aliquots were withdrawn from the oxygraph cuvette every 15 seconds, and the reaction was stopped with 3.5% (w/v) perchloric acid and 12.5 mM EDTA. The samples were then neutralized to pH 6.5

Table 1. Strains used in the study

Strain	Nuclear genotype	mtDNA	Source
MR6	*MATa ade2-1 his3-11,15 trp1-1 leu2-3,112 ura3-1 arg8::HIS3*	ρ^+	[47]
RKY62	*MATa ade2-1 his3-11,15 trp1-1 leu2-3,112 ura3-1 arg8::HIS3*	ρ^+ *atp6-K90E*	[37]
RKY61	*MATa ade2-1 his3-11,15 trp1-1 leu2-3,112 ura3-1 arg8::HIS3*	ρ^+ *atp6-P163S*	[56]
RKY62α	*MATα ade2-1 his3-11,15 trp1-1 leu2-3,112 ura3-1 arg8::HIS3*	ρ^+ *atp6-K90E*	This study
RKY61α	*MATα ade2-1 his3-11,15 trp1-1 leu2-3,112 ura3-1 arg8::HIS3*	ρ^+ *atp6-P163S*	This study
MR6-OM45GFP	*MATa ade2-1 his3-11,15 trp1-1 leu2-3,112 ura3-1 arg8::HIS3 OM45-GFP::KanMX6*	ρ^+	[37]
RKY61-OM45GFP	*MATa ade2-1 his3-11,15 trp1-1 leu2-3,112 ura3-1 arg8::HIS3 OM45-GFP::KanMX6*	ρ^+ *atp6-P163S*	[37]
KNY58	*MATa ade2-1 his3-11,15 trp1-1 leu2-3,112 ura3-1 arg8::HIS3 tim11Δ::HphNTI*	ρ^+	This study
KNY59	*MATa ade2-1 his3-11,15 trp1-1 leu2-3,112 ura3-1 arg8::HIS3 tim11Δ::HphNTI*	ρ^0	This study
KNY40	*MATa ade2-1 his3-11,15 trp1-1 leu2-3,112 ura3-1 arg8::HIS3 OM45-GFP::KanMX6*	ρ^0	This study
KNY67	*MATa ade2-1 his3-11,15 trp1-1 leu2-3,112 ura3-1 arg8::HIS3 tim11Δ::HphNTI OM45-GFP::KanMX6*	ρ^+	This study
KNY67-1	*MATa ade2-1 his3-11,15 trp1-1 leu2-3,112 ura3-1 arg8::HIS3 tim11Δ::HphNTI OM45-GFP::KanMX6*	ρ^0	This study
KNY68	*MATa/α ade2-1/ade2-1 his3-11,15/ his3-11,15 trp1-1/trp1-1 leu2-3,112/leu2-3,112 ura3-1/ura3-1 arg8::HIS3/arg8::HIS3 tim11Δ::HphNTI/TIM11*	ρ^+ *atp6-P163S*	This study
KNY69	*MATa/α ade2-1/ade2-1 his3-11,15/ his3-11,15 trp1-1/trp1-1 leu2-3,112/leu2-3,112 ura3-1/ura3-1 arg8::HIS3/arg8::HIS3 tim11Δ::HphNTI/TIM11*	ρ^+ *atp6-K90E*	This study
KNY70	*MATa/α ade2-1/ade2-1 his3-11,15/ his3-11,15 trp1-1/trp1-1 leu2-3,112/leu2-3,112 ura3-1/ura3-1 arg8::HIS3/arg8::HIS3 tim11Δ::HphNTI/TIM11 OM45-GFP::KanMX6/OM45*	ρ^+ *atp6-P163S*	This study
KNY71	*MATa/α ade2-1/ade2-1 his3-11,15/ his3-11,15 trp1-1/trp1-1 leu2-3,112/leu2-3,112 ura3-1/ura3-1 arg8::HIS3/arg8::HIS3 tim11Δ::HphNTI/TIM11 OM45-GFP::KanMX6/OM45*	ρ^+ *atp6-K90E*	This study
KNY76-1	*MATα ade2-1 his3-11,15 trp1-1 leu2-3,112 ura3-1 arg8::HIS3 tim11Δ::HphNTI*	ρ^+ *atp6-C33S-T215C*	This study
KNY88	*MATa/α ade2-1/ade2-1 his3-11,15/ his3-11,15 trp1-1/trp1-1 leu2-3,112/leu2-3,112 ura3-1/ura3-1 arg8::HIS3/arg8::HIS3 tim11Δ::HphNTI/TIM11 OM45-GFP::KanMX6/OM45*	ρ^+ *atp6-C33S-T215C*	This study
KNY89-1	*MATa ade2-1 his3-11,15 trp1-1 leu2-3,112 ura3-1 arg8::HIS3 OM45-GFP::KanMX6*	ρ^+ *atp6-C33S-T215C*	This study
KNY91-1	*MATα ade2-1 his3-11,15 trp1-1 leu2-3,112 ura3-1 arg8::HIS3*	ρ^+ *atp6-C33S-T215C*	This study
KNY103-1	*MATα ade2-1 his3-11,15 trp1-1 leu2-3,112 ura3-1 arg8::HIS3 tim11Δ::HphNTI OM45-GFP::KanMX6*	ρ^+ *atp6-C33S-T215C*	This study

by the addition of KOH and 0.3 M MOPS. The synthetized ATP was quantified using a luciferin/luciferase assay (Kinase-Glo Max Luminescence Kinase Assay, Promega) in a Beckman Coulter Paradigm plate reader. The participation of F_1F_0-ATP synthase in ATP production was assessed by measuring the sensitivity of ATP synthesis to oligomycin (3 μg/ml). The specific ATPase activity at pH 8.4 of nonosmotically protected mitochondria was measured using the procedure described by M. Somlo [45].

Measurement of the mitochondrial calcium retention capacity and swelling

A previously developed method for measurement of mitochondrial calcium retention capacity (described in detail in [37]) was used to measure the time of yPTP opening after Ca^{2+} addition. Briefly, mitochondria were diluted in CRC buffer (250 mM sucrose, 10 mM Tris-MOPS, 10 μM EGTA-Tris, 5 mM P_i-Tris, 1 mM NADH, 5 μM ETH129, 1 μM Calcium Green-5N (Thermo Fisher), 0.5 mg/ml BSA, pH 7.4) to a concentration of 500 μg/ml, and 50 μM $CaCl_2$ was added. The rapid increase in the fluorescence of Calcium Green-5N was as attributed to the release of calcium ions from the mitochondrial matrix into the buffer, likely due to the PT. Matrix swelling was evaluated by measuring optical density changes at 540 nm with a Varian Cary Bio UV-Vis spectrophotometer. Mitochondria (500 μg/ml) were suspended in 2 ml of CRC buffer without Calcium Green-5N, and then, 140 μM $CaCl_2$ and 10 μM alamethicin were added.

BN-PAGE, SDS-PAGE and Western blotting

These methods have been described previously [37]. For cross-linking experiments, mitochondria were incubated for 20 or 30 minutes at room temperature at 1 mg/ml in 250 mM sucrose, 5 mM Pi and 2 mM $CuCl_2$. Then, 5 mM N-ethylmaleimide and 5 mM EDTA were added to block the cross-linking reaction, and the incubations were transferred to ice for 10 minutes and centrifuged. Then, the ATP synthase complexes were liberated from IMM by incubation with 1.5% digitonin in extraction buffer (30 mM HEPES, 150 mM potassium acetate, 12% glycerol, 2 mM 6-aminocaproic acid, 1 mM EGTA, protease inhibitor cocktail tablets (Roche), pH 7.4) for 20 minutes and separated by BN-PAGE. Polyclonal rabbit anti-ATP synthase subunit antibodies (a gift from Marie-France Giraud, Bordeaux, France) were used.

Morphology of the mitochondria and mitochondrial network

The mitochondrial network was labelled with RFP using the pXY142-RFP plasmid encoding RFP fused to the mitochondrial targeting sequence [46]. Cells were grown at 28 or 36 °C in W0-galactose medium lacking leucine to an OD of 1 and used directly for fluorescence microscopy. The morphology of the mitochondria was assessed in whole cells grown in YPGalA medium at 28 or 36 °C to an OD of 1 and processed for electron microscopy as described previously [47]. Briefly, cells grown in YPGalA medium were fixed by incubation overnight in 2% paraformaldehyde + 2. 5% glutaraldehyde in cacodylate buffer (pH 7.4). Then, the cells were rinsed in cacodylate buffer and deionized water. Cells were immersed in 6% KMnO4 water solution for 1 hour at room temperature, rinsed 5 times in water and dehydrated in an ethanol gradient (30-100%). Then, the material was embedded in epoxy resin (Epon 812). Thin 50-nm sections were stained with 9% uranyl acetate and lead nitrate. Images were acquired using a JEM-1200 EX (Jeol, Japan) transmission electron microscope (80 keV) equipped with a MORADA camera and iTEM 1233 software.

Statistical analyses

Unless otherwise stated in the figure legends, each experiment was repeated at least three times. The intensity of the bands was quantified using ImageJ. Data are presented as the average ± s.d. or as a representative experiment. Student's t-test was used to assess significant differences with the respective control.

Results

Tim11 is essential in atp6 mutants

Our previous study indicated that the *atp6-P163S* or *atp6-K90E* mutation in the *OM45-GFP* background in *S. cerevisiae* conferred sensitivity to high calcium concentrations or hydrogen peroxide in the medium. The yPTP was desensitized to calcium in these double mutants [37]. The time of yPTP induction by calcium was longer in *atp6-P163S OM45-GFP* and *atp6-K90E OM45-GFP* mitochondria (grown at 36 °C) than in control mitochondria and comparable to the induction time in *tim11Δ* mitochondria lacking ATP synthase dimers [37]. Assuming that the hypothesis regarding the formation of the PTP core by ATP synthase dimers is true, we expected to observe an effect of the *atp6-P163S* or *atp6-K90E* mutation on yPTP induction in *tim11Δ* cells. Deletion of the *TIM11* gene not only leads to a lack of subunit *e* but also causes a lack of the *g* subunit (Supplementary Fig. S1, [22] – for all supplemental material see www.cellphysiolbiochem.com). Efforts to delete the *TIM11* gene by one-step integration of the *tim11::HphNTI* cassette into the *TIM11* locus of single *atp6-P163S*, *atp6-K90E*, and *OM45-GFP* mutants and double *atp6-P163S OM45-GFP* and *atp6-K90E OM45-GFP* mutants were ineffective. Using this method, we replaced the coding sequence of *TIM11* with the *tim11::HphNTI* cassette in a strain bearing the wild-type *ATP6* gene only. We hypothesized that Tim11 is essential in the single mutants *atp6-P163S*, *atp6-K90E*, and *OM45-GFP* and double mutants *atp6-P163S OM45-GFP* and *atp6-K90E OM45-GFP*. To verify this hypothesis, we aimed to introduce the *tim11::HphNTI* deletion into the above mutants by the classical genetic method of diploid sporulation and tetrad dissection. The *tim11::HphNTI [ρ^0]* strain was crossed with the single mutants *atp6-P163S* and *atp6-K90E* and double mutants *atp6-P163S OM45-GFP* and *atp6-K90E OM45-GFP*; the obtained diploids were sporulated, and

tetrads were dissected. Despite very efficient sporulation, only a few spores were able to grow on plates with twenty dissected tetrads (at least forty tetrads were analyzed per crossing (Supplementary Fig. S2)).

The presence of the *tim11*::*HphNTI* deletion or Om45-GFP in spores was analyzed by testing *S. cerevisiae* growth on hygromycin- or geneticin-containing plates and by evaluating GFP fluorescence. The *ATP6* gene was entirely sequenced. Surprisingly, in every spore, independent of the presence of the *tim11*::*HphNTI* deletion or Om45-GFP, the TCA codon for Atp6-S153 and the GAA codon for Atp6-E80 reverted to the wild-type CCA and AAA codons for proline and lysine, respectively, but two additional mutations appeared, leading to the substitution of the cysteine in position 23 of mature Atp6p with a serine and the threonine in position 205 with a cysteine (Atp6-C23S-T205C, designated Atp6-CSTC) (Fig. 1). Although we were not able to delete the *TIM11* gene by one-step transformation in the *OM45-GFP* strain, *OM45* was fused to *GFP* as described in [41] in *tim11*::*HphNTI* and *tim11*::*HphNTI atp6-CSTC* mutants. The lack of subunit *e* or *g* in the analyzed strains was confirmed by Western blotting with anti-Tim11 or anti-Atp20 (Supplementary Fig. S1). We therefore concluded that the Tim11 subunit, which is nonessential for the growth of *S. cerevisiae* cells even in respiratory medium, is essential in cells expressing the Atp6-P153S, Atp6-K80E, Atp6-P153S and Om45-GFP or Atp6-K80E and Om45-GFP proteins. This protein nomenclature will be used throughout the remainder of this paper.

Effect of Atp6-CSTC on growth phenotypes, mitochondrial DNA stability, the mitochondrial network and morphology

We first established the impact of Atp6-CSTC substitutions on *S. cerevisiae* growth, the stability of the mtDNA, and the morphology of the mitochondria and the mitochondrial network. Atp6-CSTC did not disturb the growth of *S. cerevisiae* cells, but in the Om45-GFP background, it led to delayed growth at elevated temperature on both fermentative and respiratory media (Fig. 2A). The Atp6-P153S or Atp6-K80E substitution in Om45-GFP led to increased sensitivity to high calcium ions concentration or hydrogen peroxide in the medium [37]. Atp6-CSTC Om45-GFP cells were also hypersensitive to calcium ions and hydrogen peroxide (Fig. 2A). These growth phenotypes of Atp6-CSTC Om45-GFP cells were suppressed by deletion of subunit *e*.

Tim11, due to its role in the dimerization of ATP synthase, is critical for cristae invaginations [9, 10]. Thus, we examined the mitochondrial network and morphology *in vivo* by fluorescence and electron microscopy, respectively. The mitochondria of cells lacking Tim11 did not form cristae. However, their inner membrane formed onion-like structures, which was the phenotype observed in cells grown at normal and elevated temperatures. Additionally, the mitochondrial network in Tim11Δ cells grown at 36 °C was not tubular, reaching all cell surface, but accumulated on one or two poles of a cell, forming long tubules close to the cell membrane (Fig. 3A; at 28 °C, this phenotype is visible only in single cells) [48, 49]. Atp6-CSTC substitutions alone did not influence the mitochondrial network but restored its defect in Tim11Δ cells (also in the Om45-GFP background; Fig. 3A). However, Atp6-CSTC substitutions did not restore the onion-like cristae morphology of mitochondria caused by Tim11 deletion, and 100% of the mitochondria of cells lacking subunit *e,* regardless of CSTC substitutions in subunit *a* and the presence of Om45-GFP, had an aberrant cristae morphology (Fig. 3B). Tim11Δ cells were also genetically unstable, with up to 60% of cells grown to late logarithmic phase at permissive temperature losing mtDNA in comparison to 3% of cells of the wild-type strain. The mtDNA instability of Tim11Δ was also partially suppressed by Atp6-CSTC substitutions (Fig. 2B). Interestingly, while the cristae morphology was normal in the Atp6-CSTC Om45-GFP double mutant, the mitochondrial network, which was normal at a permissive temperature, was hyperfused during growth at elevated temperature (Fig. 3A, B) and exhibited a phenotype much stronger than that observed in the Tim11Δ cells. Strong defects in the mitochondrial network, together with increased ROS levels and deregulation of calcium homeostasis, may contribute to the temperature sensitivity phenotype of Atp6-CSTC Om45-GFP cells.

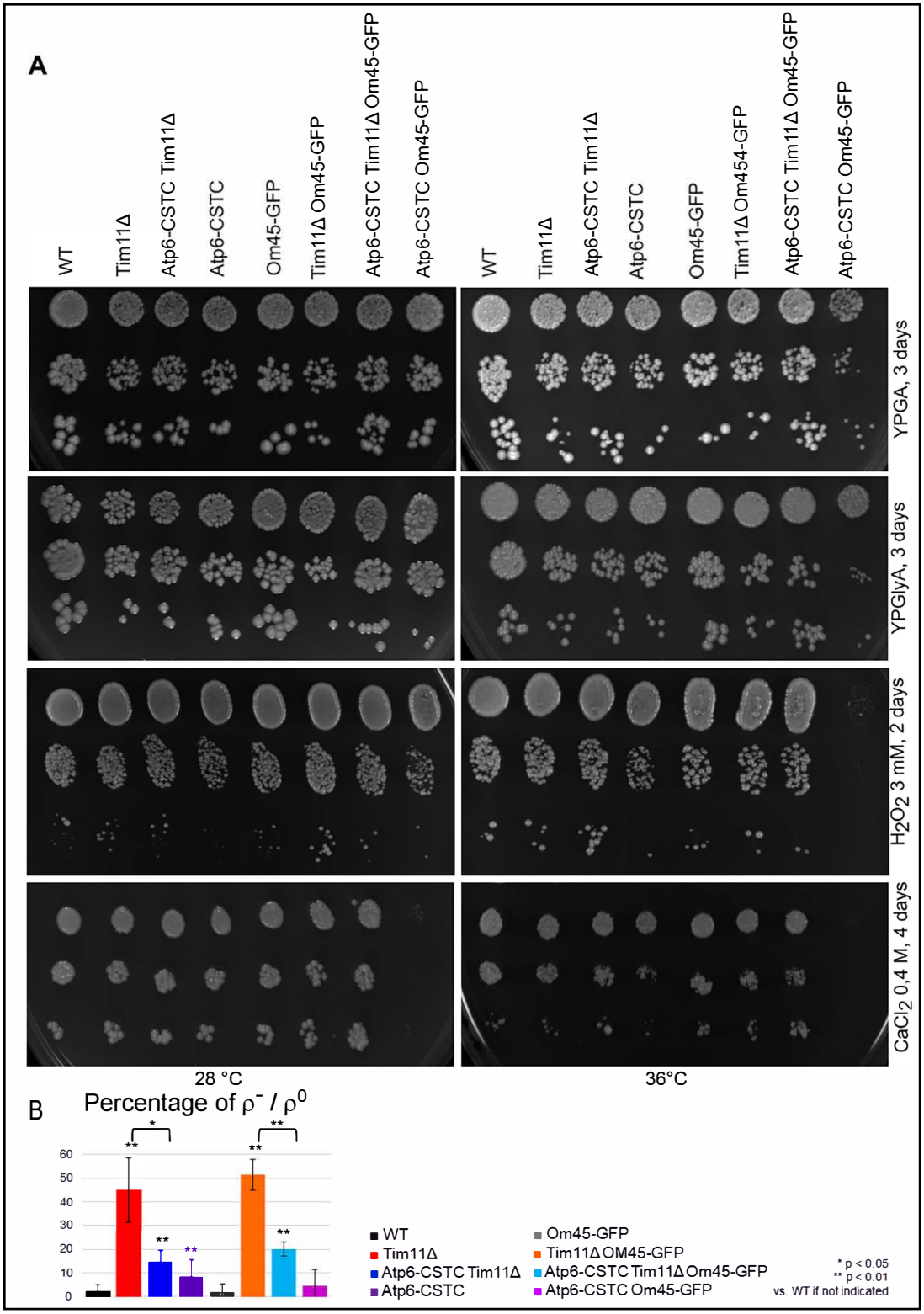

Fig. 2. Atp6-CSTC Om45-GFP cells are temperature sensitive and display hydrogen peroxide and calcium ion sensitivity suppressed by Tim11 deletion. A) Growth phenotypes. Overnight precultures were serially diluted 10-fold, spotted on plates and incubated at the indicated temperatures for 2-4 days. Representative plates are shown. B) Stability of mtDNA. Cells were grown at permissive temperature in YPGalA medium to an OD of 4. Approximately 100 cells were spread on YPGA plates and grown, and the percentage of petite colonies was counted. Experiments were performed in at least four replicates.

Atp6-CSTC restored respiration and ATP synthase activity in Tim11Δ cells

Normal respiratory growth in *S. cerevisiae* does not indicate that OXPHOS is as efficient as it is in wild-type cells. Respiratory growth defects appear only when ATP synthase activity decreases below 20% of the wild-type level [50, 51]. To explain the temperature-sensitive phenotype of the Atp6-CSTC Om45-GFP strain, we measured oxygen consumption and ATP synthesis. Mitochondria were isolated from all strains grown only at 28 °C, as culturing the Tim11Δ strain at 36 °C resulted in more than 70% petite cells. The oxygen consumption and ATP synthesis of Tim11Δ mitochondria were reduced by approximately 45 and 55%, respectively, in comparison to those of the control mitochondria, regardless of the presence of Om45-GFP (Fig. 4). Interestingly, the defect in the oxidative phosphorylation in mitochondria lacking Tim11 was suppressed by Atp6-CSTC, in both the wild-type and Om45-GFP backgrounds. Atp6-CSTC substitution alone did not influence oxygen consumption and ATP synthesis, but in combination with Om45-GFP, it reduced these activities to a level comparable to that in Tim11Δ mitochondria. Then, we measured the maximal ATPase

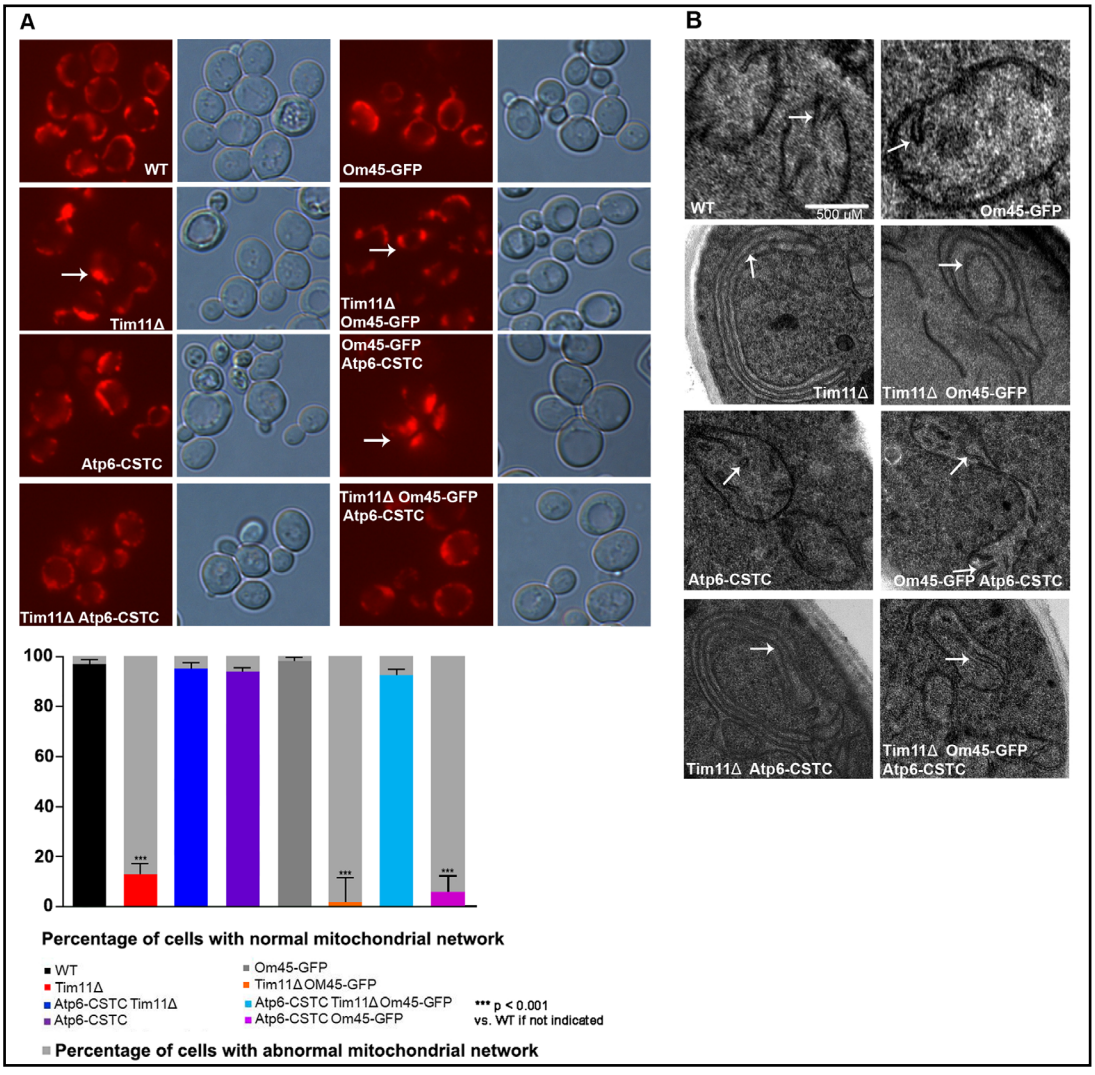

Fig. 3. Atp6-CSTC substitutions restored the mitochondrial network in Tim11Δ cells but led to the aggregation of mitochondria in Om45-GFP cells expressing Tim11. A) Cells bearing plasmids expressing RFP fused to the mitochondrial targeting sequence were grown at 36 °C in liquid W0-GalA without leucine to an OD of 1 and immediately viewed by fluorescence microscopy. B) Morphology of mitochondria in cells grown in complete galactose medium at 36 °C. Defective mitochondrial network (A) or cristae invagination (B) is shown by arrows. Representative images are shown.

activity in nonosmotically protected mitochondria buffered at pH 8.4 and in the presence of saturating amounts of ATP. A pH value of 8.4 is optimal for F_1-ATPase activity and prevents the binding of the F_1 inhibitor protein Inh1 (IF_1) to ATP synthase [52]. In all strains, the maximal ATPase activity was the same (Fig. 4, gray bars), but the oligomycin-sensitive ATPase activity varied. In the mitochondria of most strains, approximately 85% of ATPase activity was sensitive to oligomycin. However, in the single mutant Tim11Δ and double mutant Tim11Δ Om45-GFP mitochondria, the sensitivity to oligomycin decreased to approximately 60%. This indicates the reduced stability of the ATP synthase complexes. We concluded that Atp6-CSTC substitutions alone had no effect on oxygen consumption, ATP synthesis and ATP hydrolysis but restored these activities to the wild-type level in mitochondria lacking Tim11. When subunit *e* was present in the Om45-GFP background, Atp6-CSTC substitutions decreased oxygen consumption and ATP synthesis by approximately 50%. Decreased ATP synthesis may also contribute to the temperature-sensitive phenotype of Atp6-CSTC Om45-GFP cells.

Atp6-CSTC stabilized ATP synthase dimers but not by disulfide bond formation between a subunits

Subunit *e* is critical for the dimerization of ATP synthase. In the absence of this subunit, the amount of fully assembled ATP synthase was normal (as assessed here based on the amount of subunit *a*, which is immediately degraded when not assembled into the enzyme, Supplementary Fig. S1, [42, 53, 54]). However, these complexes were exclusively found in the monomeric form. The monomer of the enzyme lacking subunit *e* exhibited reduced stability [48], as indicated by the presence of free F_1 in the BN-PAGE analysis of the enzyme complexes extracted from the IMM (Fig. 5, left panel) and by the increase in ATPase activity in the presence of oligomycin (Fig. 4). Oligomycin inhibits only the coupled enzyme; therefore, oligomycin-insensitive ATP hydrolysis is carried out by free F_1 [42]. The Atp6-CSTC substitutions increased the stability of ATP synthase dimers in Tim11Δ cells (Fig. 5A, left panel) and partially restored the oligomycin-sensitive ATPase activity (Fig. 4).

To further study the impact of Atp6-CSTC substitutions on ATP synthase dimerization, we performed an analysis of ATP synthase complexes by BN-PAGE after Cu^{2+} treatment, which stabilized the dimers in Δ*e*/Δ*g* cells [22, 34, 35, 55]. Copper caused the cross-linking and stabilization of ATP synthase dimers in wild-type and Tim11Δ mitochondria (also in the Om45-GFP background) but not in those bearing Atp6-CSTC substitutions. This suggests that the cysteine at position 205 enables copper-dependent dimer stabilisation (Fig. 5, right panel). Thus, Atp6-CSTC substitutions stabilized ATP synthase dimers in cells lacking subunit *e* but not by disulfide bond formation between neighboring *a* subunits in these dimers.

Atp6-CSTC substitutions compensated for the lack of subunit e during yPTP induction

The absence of subunit *e* (and of subunit *g* as a consequence, Supplementary Fig. S1) decreased Ca^{2+} sensitivity and the conductance of the yPTP [22, 35]. We previously determined that subunit *a* mutations leading to Atp6-P153S or Atp6-K80E substitutions desensitized the yPTP to calcium in Om45-GFP mitochondria. This finding correlated with the sensitivity of cells to high calcium and hydrogen peroxide in the medium [37]. Atp6-CSTC Om45-GFP cells were also hypersensitive to calcium ions and hydrogen peroxide, suggesting that these substitutions may be significant for PT (Fig. 2A). We then asked how Atp6-CSTC substitutions influence the yPTP, especially in Tim11Δ and Om45-GFP mitochondria. For this purpose, we analyzed the rate of yPTP opening after high calcium addition by measuring the time necessary for calcium release into the buffer using the calcium retention capacity determination method. In this protocol, Ca^{2+} release occurs due to the depolarization of the membrane and therefore is compatible with the opening of a relatively small PTP [21]. Mitochondria were loaded with 50 μM $CaCl_2$, which was completely taken up into the matrix via the calcium ionophore ETH129. After 2-3 minutes, calcium was released into the buffer through the yPTP in the mitochondria of most strains, except for the single mutant Tim11Δ

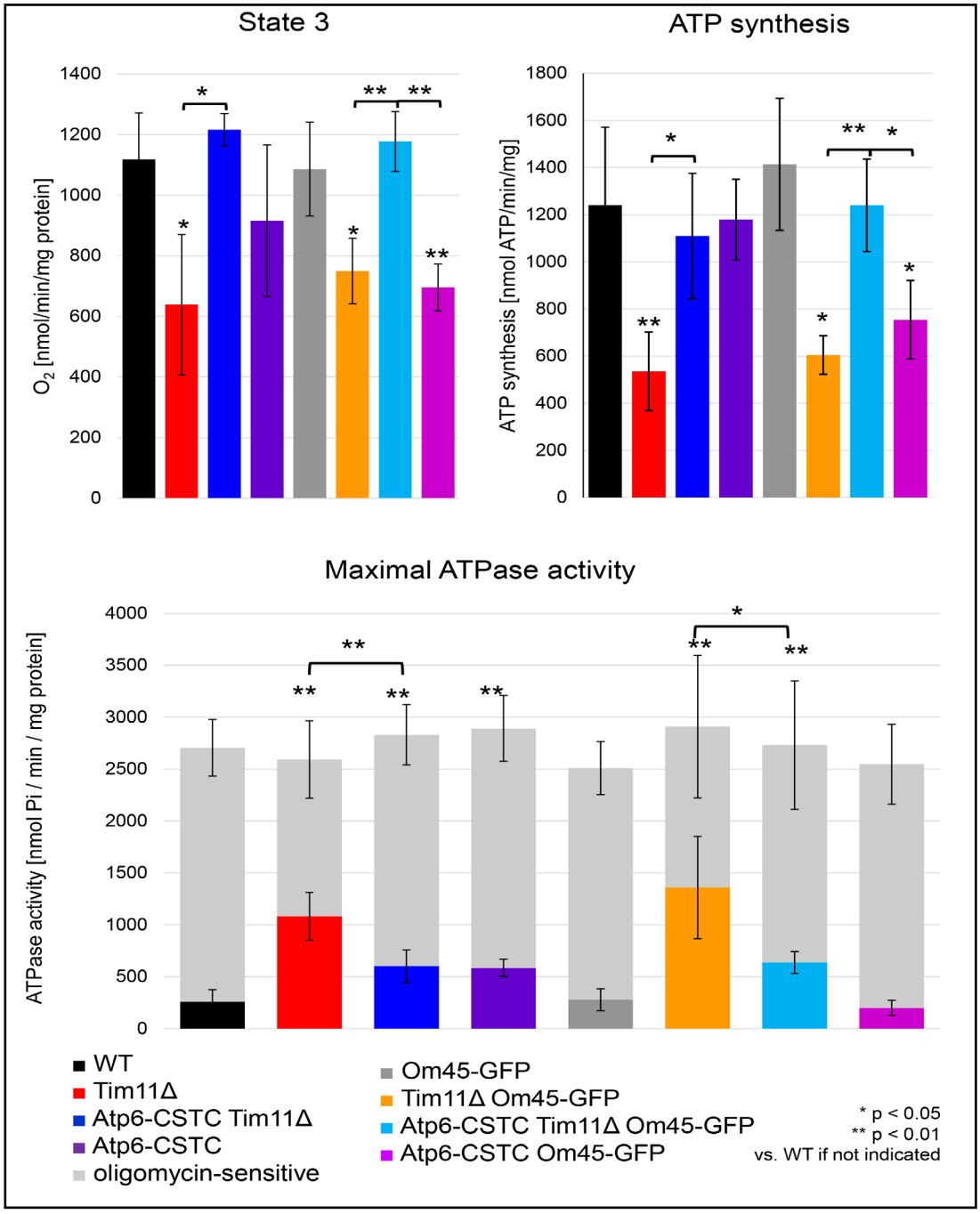

Fig. 4. State 3, ATP synthesis and ATP hydrolysis activities in mitochondria isolated from the indicated strains. Strains were grown in rich galactose medium at 28 °C. Oxygen consumption rates were measured after consecutively adding 4 mM NADH and 150 µM ADP (state 3). The rates of ATP synthesis were determined using 4 mM NADH and 750 µM ADP in the presence/absence of 20 µg of oligomycin/mg of protein. For ATPase activity, mitochondria kept at –80 °C were thawed, and the reaction was performed in the absence of osmotic protection at pH 8.4. The error bars represent standard errors calculated from at least three independent experiments, and the p values were calculated versus the wild-type control or the single mutants where indicated. In the case of ATP hydrolysis activity, p values are related to oligomycin resistant activity.

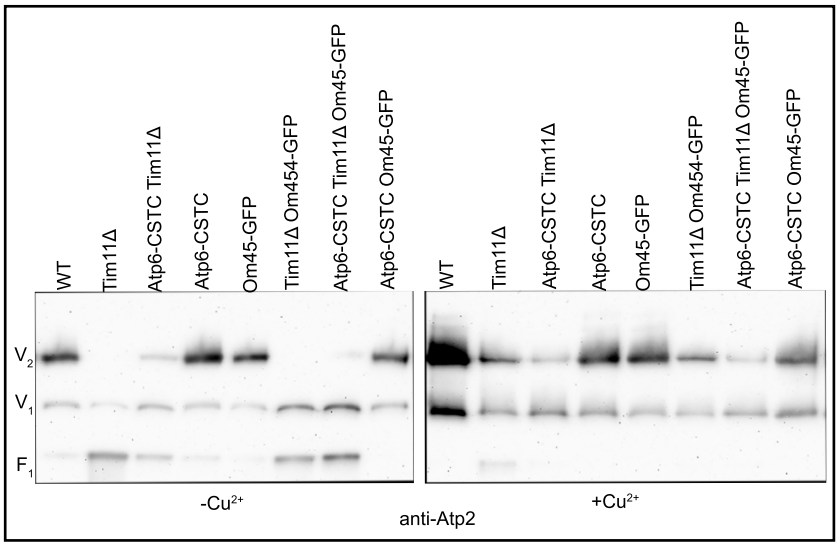

Fig. 5. Atp6-CSTC stabilizes ATP synthase dimers in the Tim11Δ cells but not through disulfide bond between *a* subunits. The steady-state ATP synthase complexes were extracted from 200 µg of mitochondria untreated (the left panel) or pretreated with 2 mM Cu^{2+} (the right panel), subjected to BN-PAGE and Western blotting with anti-Atp2 antibody. Dimeric (V_2) and monomeric (V_1) F_1F_0 complexes and free F_1 were detected by Western blotting with the indicated antibodies. Representative gels are shown.

and double mutant Tim11Δ Om45-GFP, as expected, as well as the double mutant Atp6-CSTC Om45-GFP. The time of calcium release in these mitochondria was two times longer than that in wild-type mitochondria (Fig. 6A). Thus, Atp6-CSTC substitutions restore yPTP properties in Tim11Δ cells, but in Om45-GFP cells, in which Tim11 is present, Atp6-CSTC substitutions have a contrasting effect. The Atp6-CSTC substitutions had a stronger effect on the yPTP induction delay in Om45-GFP mitochondria than Atp6-P153S or Atp6-K80E, as observed in mitochondria from cells grown at a physiological temperature of 28 °C, while the two latter substitutions delayed yPTP induction only in mitochondria isolated from cells grown at elevated temperatures [37].

Next, we measured the swelling of mitochondria induced by high (140 µM) Ca^{2+} concentrations and caused by the diffusion of sucrose into the matrix. This is only possible when a large yPTP is formed. Under this experimental condition, 60% of the wild-type mitochondria were swollen 15 minutes after calcium addition (Fig. 6B). As expected, in Tim11Δ, 25-30% of the mitochondria were swollen in both the wild-type and Om45-GFP backgrounds [22, 35]. Atp6-CSTC substitutions restored the swelling of Tim11Δ mitochondria partially in the Om45 wild-type background, increasing the fraction of swollen mitochondria to approximately 35%, and fully in Om45-GFP mitochondria, increasing the fraction of swollen mitochondria up to 75% in the Atp6-CSTC Tim11Δ Om45-GFP triple mutant. Surprisingly, in the Om45-GFP background, when subunits *e* and *g* were present and participated in stabilizing the ATP synthase dimers and yPTP, Atp6-CSTC substitutions increased the fraction of swollen mitochondria by up to 85%, although the time required for calcium release doubled (Fig. 6A). We therefore concluded that Atp6-CSTC substitutions restored the yPTP in mitochondria depleted of dimerization subunits, in terms of both its induction and conductance, in an Om45-GFP-dependent manner. The increased permeability of the mitochondrial membrane in Atp6-CSTC Om45-GFP cells may have led to their decreased growth rate at elevated temperature.

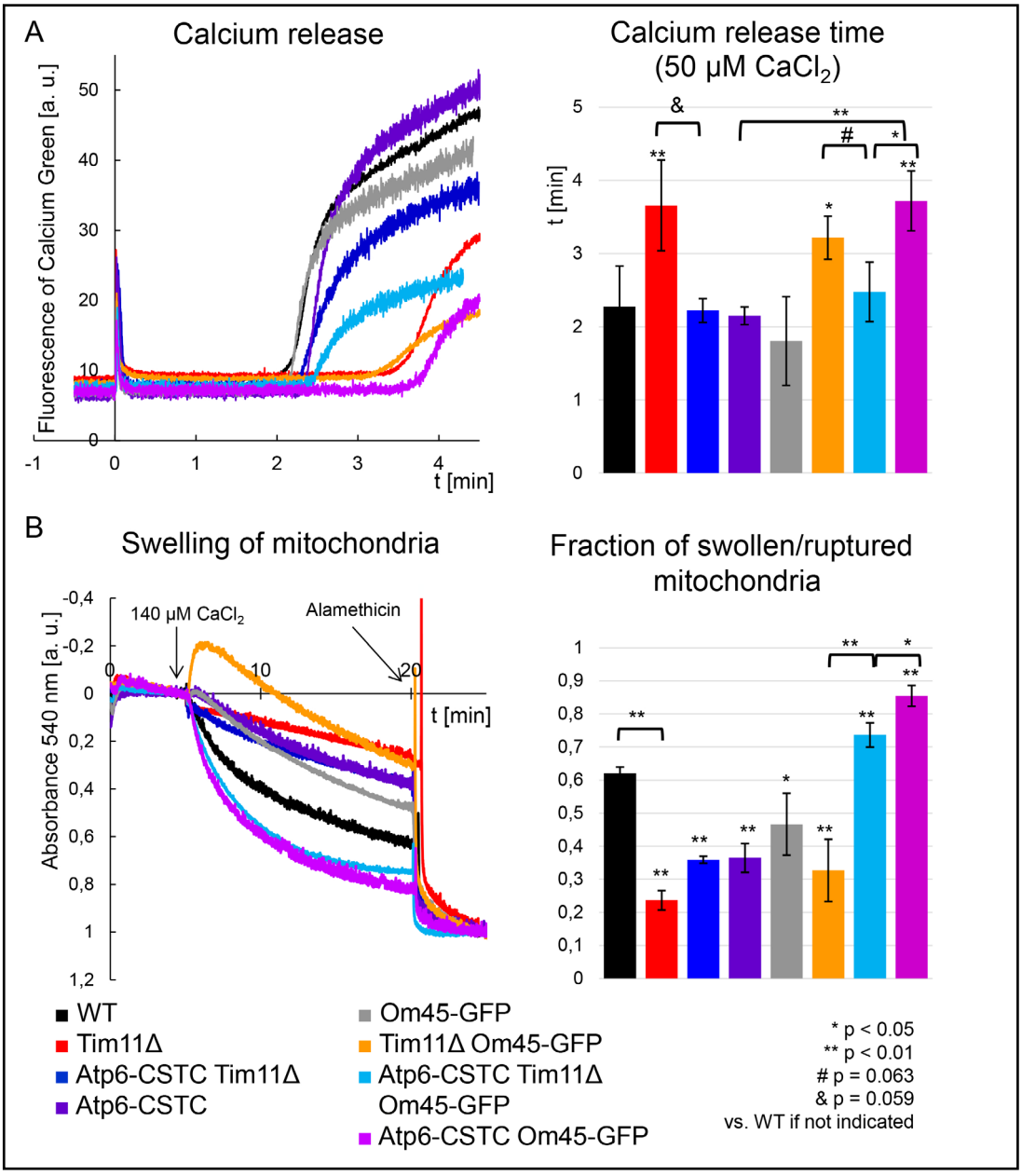

Fig. 6. Properties of the PT in yeast mitochondria. A) Time of PTP opening after calcium stimulation based on the CRC assay. Five hundred micrograms of mitochondria was suspended in CRC buffer, and 50 µM $CaCl_2$ was added at time 0 and immediately taken up by mitochondria. The time of yPTP opening was determined by a rapid increase in Calcium Green fluorescence due to calcium release into the buffer. Traces are representative of at least 5 independent experiments, and the histogram refers to the time of Ca^{2+} release. B) Mitochondrial swelling assay. Swelling was induced by the addition of 140 µM $CaCl_2$ to mitochondria suspended in CRC buffer and measured as the decrease in absorbance at 540 nm. Alamethicin (10 µM) was added after 15 minutes of swelling for normalization of the experiment. The fraction of swollen mitochondria after yPTP opening was calculated using maximal swelling induced by alamethicin as 1. Traces are representative of at least 5 independent experiments, and the histogram refers to the fraction of swollen mitochondria 15 minutes after $CaCl_2$ addition. Statistical significance is indicated.

Discussion

This paper extends the research on ATP synthase and its function as the PTP core, a subject that is currently under discussion in the literature [21]. We previously reported that the Atp6-P153S or Atp6-K80E substitution in Om45-GFP cells in *S. cerevisiae* led to calcium and ROS homeostasis deregulation and delayed the induction of yPTP by calcium, while OXPHOS functioned normally. Moreover, we have shown that the addition of calcium to mitochondria induced the formation of dimeric and oligomeric complexes of ATP synthase during yPTP formation, and P153S and K80E amino acid substitutions in subunit *a* modulated this process in an Om45-dependent manner [37]. We describe here another example of amino acid substitutions in the *a* subunit, namely, Atp6-C23S-T205C, which modulate the induction and conductance of yPTP. These two substitutions were selected *in vivo* as spontaneous suppressors in Atp6-P153S, Atp6-K80E, Atp6-P153S Om45-GFP and Atp6-K80E Om45-GFP cells [37], in which we additionally tried to delete subunit *e*. Interestingly, *S. cerevisiae* cells reverted the original Atp6-P153S or Atp6-K80E amino acid substitution to the wild-type amino acid and "moved" the cysteine from position 23 to position 205 of the Atp6 sequence. The absence of subunits *e* and *g* had no effect on the growth of *S. cerevisiae* cells but led to a lack of ATP synthase dimers and drastically reduced yPTP conductance [35]. In *S. cerevisiae*, ATP synthase dimers are stabilized by the formation of disulfide bonds between the cysteine residues in adjacent *a* subunits of two monomers, which also occurs in cells lacking the *e* and *g* subunits (Fig. 1, Fig. 5; [35]). These genetic results indicate that yPTP function is important for the fitness of *S. cerevisiae* cells. Complete yPTP dysfunction, a situation possible when Atp6-P153S or Atp6-K80E is combined with the absence of subunit *e* or *g*, is lethal. Unfortunately, we could not verify this hypothesis experimentally.

We analyzed the effects of Atp6-CSTC substitutions on ATP synthase activities and yPTP formation. The transfer of the cysteine from position 23 to 205 suppressed the defects caused by a lack of ATP synthase dimerization subunits. Indeed, these substitutions (i) improved the stability of the mitochondrial genome; (ii) restored the mitochondrial network but not its morphology; (iii) stabilized the ATP synthase dimers and monomers and improved enzyme function by restoring oxygen consumption and ATP synthesis to the wild-type level; and (iv) restored the yPTP induction time to the wild-type level and increased yPTP conduction. These results prove that Atp6-P153 and Atp6-K80 are, similar to subunit *e*, important for ATP synthase dimer stabilization.

Markedly, Atp6-CSTC substitutions have deleterious effects on *S. cerevisiae* cells in the presence of stable ATP synthase dimers in the Om45-GFP background, similar to Atp6-P153S and Atp6-K80E [37]. Atp6-CSTC in the Om45-GFP background had even stronger effects. These cells were not only sensitive to hydrogen peroxide or high concentrations of calcium but also temperature sensitive when grown on fermentative medium. In these cells, the oxygen consumption and ATP synthesis was reduced to 50% at physiological growth temperature, while in Atp6-P153S Om45-GFP mitochondria only at elevated growth temperature [37]. Interestingly, although yPTP opening is desensitized to calcium in Atp6-CSTC Om45-GFP cells, even more than in Atp6-P153S Om45-GFP and Atp6-K80E Om45-GFP, its conductance for sucrose is higher in Atp6-CSTC Om45-GFP than in the wild-type and Atp6-P153S Om45-GFP cells (Supplementary Fig. S3B). Taking into account the fact that the mitochondrial network at elevated growth temperatures is aggregated in Atp6-CSTC Om45-GFP, as in Atp6-P153S Om45-GFP (Supplementary Fig. S3A), while Atp6-P153S Om45-GFP mitochondria swell normally at permissive temperatures (Supplementary Fig. S3B) and slightly slower than wild-type mitochondria at elevated temperatures [37, 56], we propose that the increased conductance of the yPTP in Atp6-CSTC Om45-GFP cells contributes to the temperature-sensitive growth phenotype, which is absent in Atp6-P153S Om45-GFP cells. The yPTP function is therefore critical for *S. cerevisiae* cell fitness when overactivated (especially at elevated temperature). The results presented here argue that subunit *a* has a direct role in yPTP formation together with subunits *e* and *g* and the first transmembrane

helix of subunit *b* [35]. Subunit *a* modulates yPTP induction by calcium ions, which we have shown previously [37], and yPTP conductance, which we show here (Fig. 6B, Fig. 7).

The results presented in this paper are very important in the current debate regarding the role of ATP synthase in PT, particularly because these results have been obtained *in vivo*. There is evidence that PT is an evolutionarily conserved process between yeasts and mammals [32, 57]. Understanding how the channel operates and its composition and regulation are important objectives for medicine. Indeed, there is much data in the literature showing that abnormal PTP function plays a role in diseases and pathological conditions, including myopathies, Parkinson's disease, diabetic encephalopathy, cardiomyopathy, and ischemia/reperfusion [58-63]. Furthermore, mutations in the *MT-ATP6* gene, encoding ATP synthase subunit *a*, in addition to their presence in cancer samples [64, 65], are the cause of myopathies, such as neurogenic ataxia retinitis pigmentosa (NARP; [66, 67]), maternally inherited Leigh syndrome (MILS; [68-70]), mitochondrial encephalomyopathy, lactic acidosis, stroke-like episodes (MELAS; [71]), and other diseases, including cardiomyopathies [72]. Whether the role of subunit *a* in PTP regulation described here plays a role in the pathogenesis of this group of diseases is an intriguing possibility that warrants further study.

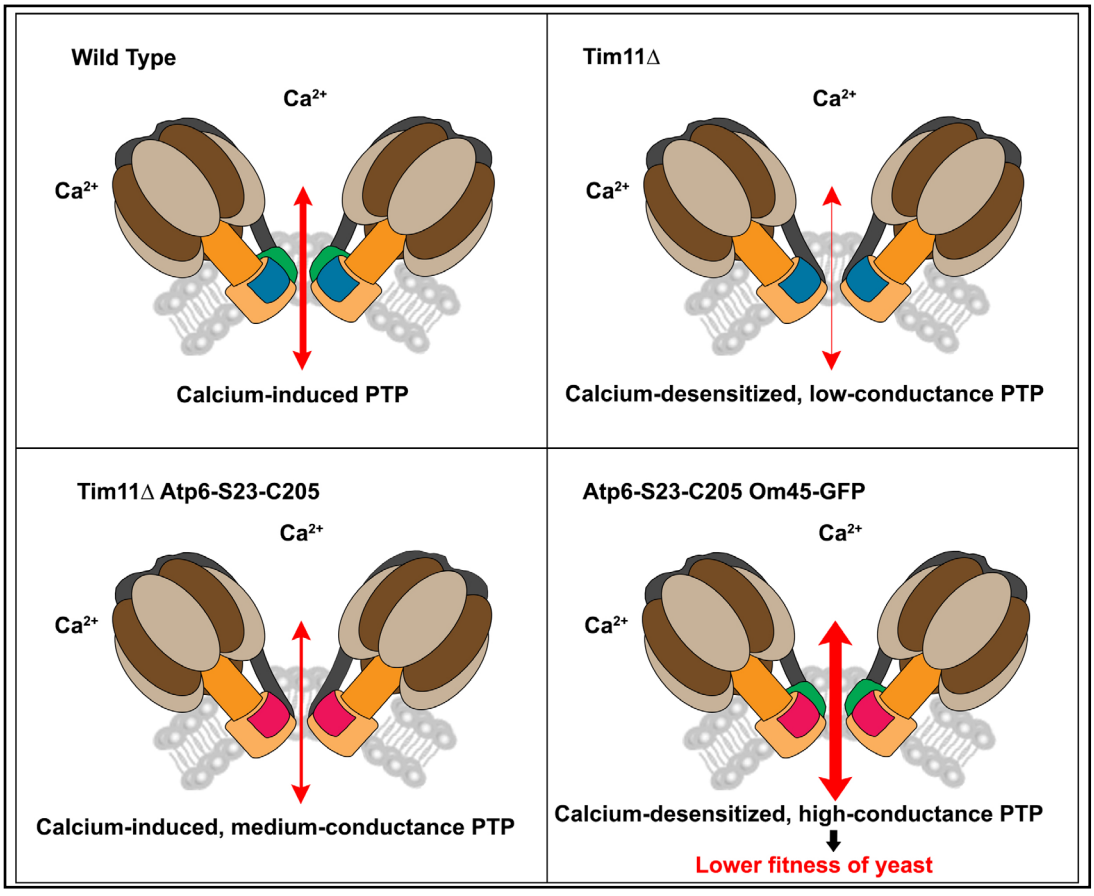

Fig. 7. Illustration of the yPTP in Atp6-CSTC cells based on the presented results. Lack of the dimerization subunits of ATP synthase (marked in green) leads to calcium-desensitized low-conductance yPTP (the upper right panel). The substitutions Atp6-K80E or Atp6-P153S in subunit *a* in the Om45-GFP background also lead to calcium-desensitized channels but with normal conductance (Fig. S3B, [37]). The function of subunit *e* is essential in these cells, as its deletion was not possible. During *TIM11* gene deletion selection of compensatory mutations occurred, resulting in C23S and T205C residue substitutions in the Atp6. This Atp6 variant (marked in purple) compensates for the lack of subunit *e* during yPTP formation, increasing its conductance partially in the Om45 background (the lower left panel) but above the normal conductance in the Om45-GFP background (the lower right panel). This high-conductance channel, induced by increased calcium and ROS levels, contributes to the heat sensitivity of Atp6-CSTC Om45-GFP yeast cells.

Acknowledgements

RK thanks Prof. P. Bernardi for critically reading the manuscript. The authors thank the Laboratory of Electron Microscopy of Mossakowski Medical Research Centre of PAS for the mitochondrial morphology analysis.

Statement of Ethics

The permission number for work with genetically modified microorganisms (GMM I) for RK is 01.2-28/201.

Funding

This work was supported by a grant from the National Science Center of Poland (2016/23/B/NZ3/02098) to RK.

Author Contributions

KN isolated suppressors, constructed the strains, isolated mitochondria, performed the CRC and swelling experiments and protein electrophoresis, and prepared figures; EB isolated mitochondria and performed respiration and ATP synthase activity assays and protein electrophoresis; CP performed phenotypic analysis and respiration measurements and prepared figures; RK designed the work, wrote the original draft of the manuscript, and prepared figures; all authors participated in the review and editing of the manuscript.

Disclosure Statement

The authors declare that they have no competing or financial interests.

References

1 Guo H, Bueler SA, Rubinstein JL: Atomic model for the dimeric FO region of mitochondrial ATP synthase. Science 2017;358:936-940.
2 Rubinstein JL, Walker JE, Henderson R: Structure of the mitochondrial ATP synthase by electron cryomicroscopy. EMBO J 2003;22:6182-6192.
3 Mitchell P, Moyle J: Chemiosmotic hypothesis of oxidative phosphorylation. Nature 1967;213:137-139.
4 Pogoryelov D, Krah A, Langer JD, Yildiz O, Faraldo-Gomez JD, Meier T: Microscopic rotary mechanism of ion translocation in the F(o) complex of ATP synthases. Nature Chem Biol 2010;6:891-899.
5 Vik SB, Antonio BJ: A mechanism of proton translocation by F1F0 ATP synthases suggested by double mutants of the a subunit. J Biol Chem 1994;269:30364-30369.
6 Boyer PD: The binding change mechanism for ATP synthase--some probabilities and possibilities. Biochim Biophys Acta 1993;1140:215-250.
7 Abrahams JP, Leslie AG, Lutter R, Walker JE: Structure at 2.8 A resolution of F1-ATPase from bovine heart mitochondria. Nature 1994;370:621-628.
8 Hahn A, Parey K, Bublitz M, Mills DJ, Zickermann V, Vonck J, Kuhlbrandt W, Meier T: Structure of a Complete ATP Synthase Dimer Reveals the Molecular Basis of Inner Mitochondrial Membrane Morphology. Mol Cell 2016;63:445-456.
9 Davies KM, Anselmi C, Wittig I, Faraldo-Gomez JD, Kuhlbrandt W: Structure of the yeast F1Fo-ATP synthase dimer and its role in shaping the mitochondrial cristae. Proc Natl Acad Sci U S A 2012;109:13602-13607.
10 Paumard P, Vaillier J, Coulary B, Schaeffer J, Soubannier V, Mueller DM, Brethes D, di Rago JP, Velours J: The ATP synthase is involved in generating mitochondrial cristae morphology. EMBO J 2002;21:221-230.
11 Habersetzer J, Larrieu I, Priault M, Salin B, Rossignol R, Brethes D, Paumard P: Human F1F0 ATP synthase, mitochondrial ultrastructure and OXPHOS impairment: a (super-)complex matter? PloS One 2013;8:e75429.

12 Alavian KN, Beutner G, Lazrove E, Sacchetti S, Park HA, Licznerski P, Li H, Nabili P, Hockensmith K, Graham M, Porter GA, Jr., Jonas EA: An uncoupling channel within the c-subunit ring of the F1FO ATP synthase is the mitochondrial permeability transition pore. Proc Natl Acad Sci U S A 2014;111:10580-10585.
13 Bonora M, Bononi A, De Marchi E, Giorgi C, Lebiedzinska M, Marchi S, Patergnani S, Rimessi A, Suski JM, Wojtala A, Wieckowski MR, Kroemer G, Galluzzi L, Pinton P: Role of the c subunit of the FO ATP synthase in mitochondrial permeability transition. Cell Cycle 2013;12:674-683.
14 Giorgio V, von Stockum S, Antoniel M, Fabbro A, Fogolari F, Forte M, Glick GD, Petronilli V, Zoratti M, Szabo I, Lippe G, Bernardi P: Dimers of mitochondrial ATP synthase form the permeability transition pore. Proc Natl Acad Sci U S A 2013;110:5887-5892.
15 Bernardi P, Rasola A, Forte M, Lippe G: The Mitochondrial Permeability Transition Pore: Channel Formation by F-ATP Synthase, Integration in Signal Transduction, and Role in Pathophysiology. Physiol Rev 2015;95:1111-1155.
16 Ichas F, Jouaville LS, Mazat JP: Mitochondria are excitable organelles capable of generating and conveying electrical and calcium signals. Cell 1997;89:1145-1153.
17 Zorov DB, Juhaszova M, Sollott SJ: Mitochondrial reactive oxygen species (ROS) and ROS-induced ROS release. Physiol Rev 2014;94:909-950.
18 Maximilian Buja L: Mitochondria in Ischemic Heart Disease. Adv Exp Med Biol 2017;982:127-140.
19 Rasola A, Bernardi P: The mitochondrial permeability transition pore and its adaptive responses in tumor cells. Cell Calcium 2014;56:437-445.
20 He J, Ford HC, Carroll J, Ding S, Fearnley IM, Walker JE: Persistence of the mitochondrial permeability transition in the absence of subunit c of human ATP synthase. Proc Natl Acad Sci U S A 2017;114:3409-3414.
21 Bernardi P: Why F-ATP Synthase Remains a Strong Candidate as the Mitochondrial Permeability Transition Pore. Front Physiol 2018;9:1543.
22 Carraro M, Giorgio V, Sileikyte J, Sartori G, Forte M, Lippe G, Zoratti M, Szabo I, Bernardi P: Channel formation by yeast F-ATP synthase and the role of dimerization in the mitochondrial permeability transition. J Biol Chem 2014;289:15980-15985.
23 von Stockum S, Giorgio V, Trevisan E, Lippe G, Glick GD, Forte MA, Da-Re C, Checchetto V, Mazzotta G, Costa R, Szabo I, Bernardi P: F-ATPase of Drosophila melanogaster forms 53-picosiemen (53-pS) channels responsible for mitochondrial Ca2+-induced Ca2+ release. J Biol Chem 2015;290:4537-4544.
24 Szabo I, Zoratti M: Mitochondrial channels: ion fluxes and more. Physiol Rev 2014;94:519-608.
25 Urbani A, Giorgio V, Carrer A, Franchin C, Arrigoni G, Jiko C, Abe K, Maeda S, Shinzawa-Itoh K, Bogers JFM, McMillan DGG, Gerle C, Szabo I, Bernardi P: Purified F-ATP synthase forms a Ca(2+)-dependent high-conductance channel matching the mitochondrial permeability transition pore. Nat Commun 2019;10:4341.
26 Mnatsakanyan N, Llaguno MC, Yang Y, Yan Y, Weber J, Sigworth FJ, Jonas EA: A mitochondrial megachannel resides in monomeric F1FO ATP synthase. Nat Commun 2019;10:5823.
27 Bonora M, Morganti C, Morciano G, Pedriali G, Lebiedzinska-Arciszewska M, Aquila G, Giorgi C, Rizzo P, Campo G, Ferrari R, Kroemer G, Wieckowski MR, Galluzzi L, Pinton P: Mitochondrial permeability transition involves dissociation of F1FO ATP synthase dimers and C-ring conformation. EMBO Rep 2017;18:1077-1089.
28 Giorgio V, Burchell V, Schiavone M, Bassot C, Minervini G, Petronilli V, Argenton F, Forte M, Tosatto S, Lippe G, Bernardi P: Ca(2+) binding to F-ATP synthase beta subunit triggers the mitochondrial permeability transition. EMBO Rep 2017;18:1065-1076.
29 Johnson KM, Chen X, Boitano A, Swenson L, Opipari AW, Jr., Glick GD: Identification and validation of the mitochondrial F1F0-ATPase as the molecular target of the immunomodulatory benzodiazepine Bz-423. Chem Biol 2005;12:485-496.
30 Antoniel M, Jones K, Antonucci S, Spolaore B, Fogolari F, Petronilli V, Giorgio V, Carraro M, Di Lisa F, Forte M, Szabo I, Lippe G, Bernardi P: The unique histidine in OSCP subunit of F-ATP synthase mediates inhibition of the permeability transition pore by acidic pH. EMBO Rep 2018;19:257-268.
31 Neginskaya MA, Solesio ME, Berezhnaya EV, Amodeo GF, Mnatsakanyan N, Jonas EA, Pavlov EV: ATP Synthase C-Subunit-Deficient Mitochondria Have a Small Cyclosporine A-Sensitive Channel, but Lack the Permeability Transition Pore. Cell Rep 2019;26:11-17 e12.

32 Kamei Y, Koushi M, Aoyama Y, Asakai R: The yeast mitochondrial permeability transition is regulated by reactive oxygen species, endogenous Ca(2+) and Cpr3, mediating cell death. Biochim Biophys Acta Bioenerg 2018;1859:1313-1326.
33 Gutierrez-Aguilar M, Uribe-Carvajal S: The mitochondrial unselective channel in Saccharomyces cerevisiae. Mitochondrion 2015;22:85-90.
34 Velours J, Stines-Chaumeil C, Habersetzer J, Chaignepain S, Dautant A, Brethes D: Evidence of the proximity of ATP synthase subunits 6 (a) in the inner mitochondrial membrane and in the supramolecular forms of Saccharomyces cerevisiae ATP synthase. J Biol Chem 2011;286:35477-35484.
35 Carraro M, Checchetto V, Sartori G, Kucharczyk R, di Rago JP, Minervini G, Franchin C, Arrigoni G, Giorgio V, Petronilli V, Tosatto SCE, Lippe G, Szabo I, Bernardi P: High-Conductance Channel Formation in Yeast Mitochondria is Mediated by F-ATP Synthase e and g Subunits. Cell Physiol Biochem 2018;50:1840-1855.
36 Zeng X, Neupert W, Tzagoloff A: The metalloprotease encoded by ATP23 has a dual function in processing and assembly of subunit 6 of mitochondrial ATPase. Mol Biol Cell 2007;18:617-626.
37 Niedzwiecka K, Tisi R, Penna S, Lichocka M, Plochocka D, Kucharczyk R: Two mutations in mitochondrial ATP6 gene of ATP synthase, related to human cancer, affect ROS, calcium homeostasis and mitochondrial permeability transition in yeast. Biochim Biophys Acta Mol Cell Res 2018;1865:117-131.
38 Lauffer S, Mabert K, Czupalla C, Pursche T, Hoflack B, Rodel G, Krause-Buchholz U: Saccharomyces cerevisiae porin pore forms complexes with mitochondrial outer membrane proteins Om14p and Om45p. J Biol Chem 2012;287:17447-17458.
39 Herskowitz I, Jensen RE: Putting the HO gene to work: practical uses for mating-type switching. Meth Enzym 1991;194:132-146.
40 Wysocka-Kapcinska M, Torocsik B, Turiak L, Tsaprailis G, David CL, Hunt AM, Vekey K, Adam-Vizi V, Kucharczyk R, Chinopoulos C: The suppressor of AAC2 Lethality SAL1 modulates sensitivity of heterologously expressed artemia ADP/ATP carrier to bongkrekate in yeast. PloS One 2013;8:e74187.
41 Kanki T, Kang D, Klionsky DJ: Monitoring mitophagy in yeast: the Om45-GFP processing assay. Autophagy 2009;5:1186-1189.
42 Kucharczyk R, Salin B, di Rago JP: Introducing the human Leigh syndrome mutation T9176G into Saccharomyces cerevisiae mitochondrial DNA leads to severe defects in the incorporation of Atp6p into the ATP synthase and in the mitochondrial morphology. Hum Mol Genet 2009;18:2889-2898.
43 Guerin B, Labbe P, Somlo M: Preparation of yeast mitochondria (Saccharomyces cerevisiae) with good P/O and respiratory control ratios. Meth Enzym 1979;55:149-159.
44 Rigoulet M, Guerin B: Phosphate transport and ATP synthesis in yeast mitochondria: effect of a new inhibitor: the tribenzylphosphate. FEBS Lett 1979;102:18-22.
45 Somlo M: Induction and repression of mitochondrial ATPase in yeast. Eur J Biochem 1968;5:276-284.
46 Westermann B, Neupert W: Mitochondria-targeted green fluorescent proteins: convenient tools for the study of organelle biogenesis in Saccharomyces cerevisiae. Yeast 2000;16:1421-1427.
47 Rak M, Tetaud E, Godard F, Sagot I, Salin B, Duvezin-Caubet S, Slonimski PP, Rytka J, di Rago JP: Yeast cells lacking the mitochondrial gene encoding the ATP synthase subunit 6 exhibit a selective loss of complex IV and unusual mitochondrial morphology. J Biol Chem 2007;282:10853-10864.
48 Everard-Gigot V, Dunn CD, Dolan BM, Brunner S, Jensen RE, Stuart RA: Functional analysis of subunit e of the F1Fo-ATP synthase of the yeast Saccharomyces cerevisiae: importance of the N-terminal membrane anchor region. Eukaryot Cell 2005;4:346-355.
49 Westermann B: Bioenergetic role of mitochondrial fusion and fission. Biochim Biophys Acta 2012;1817:1833-1838.
50 Mukhopadhyay A, Uh M, Mueller DM: Level of ATP synthase activity required for yeast Saccharomyces cerevisiae to grow on glycerol media. FEBS Lett 1994;343:160-164.
51 Kucharczyk R, Ezkurdia N, Couplan E, Procaccio V, Ackerman SH, Blondel M, di Rago JP: Consequences of the pathogenic T9176C mutation of human mitochondrial DNA on yeast mitochondrial ATP synthase. Biochim Biophys Acta 2010;1797:1105-1112.
52 Venard R, Brethes D, Giraud MF, Vaillier J, Velours J, Haraux F: Investigation of the role and mechanism of IF1 and STF1 proteins, twin inhibitory peptides which interact with the yeast mitochondrial ATP synthase. Biochemistry 2003;42:7626-7636.

53 Lefebvre-Legendre L, Vaillier J, Benabdelhak H, Velours J, Slonimski PP, di Rago JP: Identification of a nuclear gene (FMC1) required for the assembly/stability of yeast mitochondrial F(1)-ATPase in heat stress conditions. J Biol Chem 2001;276:6789-6796.
54 Rak M, Zeng X, Briere JJ, Tzagoloff A: Assembly of F0 in Saccharomyces cerevisiae. Biochim Biophys Acta 2009;1793:108-116.
55 Fronzes R, Weimann T, Vaillier J, Velours J, Brethes D: The peripheral stalk participates in the yeast ATP synthase dimerization independently of e and g subunits. Biochemistry 2006;45:6715-6723.
56 Niedzwiecka K, Kabala AM, Lasserre JP, Tribouillard-Tanvier D, Golik P, Dautant A, di Rago JP, Kucharczyk R: Yeast models of mutations in the mitochondrial ATP6 gene found in human cancer cells. Mitochondrion 2016;29:7-17.
57 Azzolin L, von Stockum S, Basso E, Petronilli V, Forte MA, Bernardi P: The mitochondrial permeability transition from yeast to mammals. FEBS Lett 2010;584:2504-2509.
58 Sileikyte J, Forte M: The Mitochondrial Permeability Transition in Mitochondrial Disorders. Oxid Med Cell Longev 2019;2019:3403075.
59 Ludtmann MHR, Angelova PR, Horrocks MH, Choi ML, Rodrigues M, Baev AY, Berezhnov AV, Yao Z, Little D, Banushi B, Al-Menhali AS, Ranasinghe RT, Whiten DR, Yapom R, Dolt KS, Devine MJ, Gissen P, Kunath T, Jaganjac M, et al.: alpha-synuclein oligomers interact with ATP synthase and open the permeability transition pore in Parkinson's disease. Nat Commun 2018;9:2293.
60 Yan S, Du F, Wu L, Zhang Z, Zhong C, Yu Q, Wang Y, Lue LF, Walker DG, Douglas JT, Yan SS: F1F0 ATP Synthase-Cyclophilin D Interaction Contributes to Diabetes-Induced Synaptic Dysfunction and Cognitive Decline. Diabetes 2016;65:3482-3494.
61 Fernandez-Sanz C, Ruiz-Meana M, Castellano J, Miro-Casas E, Nunez E, Inserte J, Vazquez J, Garcia-Dorado D: Altered FoF1 ATP synthase and susceptibility to mitochondrial permeability transition pore during ischaemia and reperfusion in aging cardiomyocytes. Throm Hem 2015;113:441-451.
62 Halestrap AP, Richardson AP: The mitochondrial permeability transition: a current perspective on its identity and role in ischaemia/reperfusion injury. J Mol Cell Cardiol 2015;78:129-141.
63 Angelin A, Bonaldo P, Bernardi P: Altered threshold of the mitochondrial permeability transition pore in Ullrich congenital muscular dystrophy. Biochim Biophys Acta 2008;1777:893-896.
64 Jarviaho T, Hurme-Niiranen A, Soini HK, Niinimaki R, Mottonen M, Savolainen ER, Hinttala R, Harila-Saari A, Uusimaa J: Novel non-neutral mitochondrial DNA mutations found in childhood acute lymphoblastic leukemia. Clin Genet 2018;93:275-285.
65 Li L, Chen L, Li J, Zhang W, Liao Y, Chen J, Sun Z: Correlational study on mitochondrial DNA mutations as potential risk factors in breast cancer. Oncotarget 2016;7:31270-31283.
66 Duno M, Wibrand F, Baggesen K, Rosenberg T, Kjaer N, Frederiksen AL: A novel mitochondrial mutation m.8989G>C associated with neuropathy, ataxia, retinitis pigmentosa - the NARP syndrome. Gene 2013;515:372-375.
67 Baracca A, Barogi S, Carelli V, Lenaz G, Solaini G: Catalytic activities of mitochondrial ATP synthase in patients with mitochondrial DNA T8993G mutation in the ATPase 6 gene encoding subunit a. J Biol Chem 2000;275:4177-4182.
68 Schon EA, Santra S, Pallotti F, Girvin ME: Pathogenesis of primary defects in mitochondrial ATP synthesis. Semin Cell Dev Biol 2001;12:441-448.
69 Uittenbogaard M, Brantner CA, Fang Z, Wong LC, Gropman A, Chiaramello A: Novel insights into the functional metabolic impact of an apparent de novo m.8993T>G variant in the MT-ATP6 gene associated with maternally inherited form of Leigh Syndrome. Mol Genet Metab 2018;124:71-81.
70 Akagi M, Inui K, Tsukamoto H, Sakai N, Muramatsu T, Yamada M, Matsuzaki K, Goto Y, Nonaka I, Okada S: A point mutation of mitochondrial ATPase 6 gene in Leigh syndrome. Neuromuscul Disord 2002;12:53-55.
71 Aure K, Dubourg O, Jardel C, Clarysse L, Sternberg D, Fournier E, Laforet P, Streichenberger N, Petiot P, Gervais-Bernard H, Vial C, Bedat-Millet AL, Drouin-Garraud V, Bouillaud F, Vandier C, Fontaine B, Lombes A: Episodic weakness due to mitochondrial DNA MT-ATP6/8 mutations. Neurology 2013;81:1810-1818.
72 Dautant A, Meier T, Hahn A, Tribouillard-Tanvier D, di Rago JP, Kucharczyk R: ATP Synthase Diseases of Mitochondrial Genetic Origin. Front Physiol 2018;9:329.